

Journal of Biomedical Optics

SPIEDigitalLibrary.org/jbo

Effect of measurement on the ballistic–diffusive transition in turbid media

Ziv Glasser
Andre Yaroshevsky
Bavat Barak
Er’el Granot
Shmuel Sternklar

Effect of measurement on the ballistic–diffusive transition in turbid media

Ziv Glasser, Andre Yaroshevsky, Bavat Barak, Er'el Granot, and Shmuel Sternklar

Ariel University, Department of Electrical and Electronic Engineering, Kiryat Hamada 4, Ariel 40700, Israel

Abstract. The dependence of the transition between the ballistic and the diffusive regimes of turbid media on the experimental solid angle of the detection system is analyzed theoretically and experimentally. A simple model is developed which shows the significance of experimental conditions on the location of the ballistic–diffusive transition. It is demonstrated that decreasing the solid angle expands the ballistic regime; however, this benefit is bounded by the initial Gaussian beam diffraction. In addition, choosing the appropriate wavelength according to the model's principles provides another means of expanding the ballistic regime. Consequently, by optimizing the experimental conditions, it should be possible to extract the ballistic image of a tissue with a thickness of 1 cm. © 2013 Society of Photo-Optical Instrumentation Engineers (SPIE) [DOI: 10.1117/1.JBO.18.10.106006]

Keywords: biomedical optics; illumination; diffusion; scattering; tissues; collimators.

Paper 130330RR received May 9, 2013; revised manuscript received Sep. 3, 2013; accepted for publication Sep. 5, 2013; published online Oct. 8, 2013.

1 Introduction

In tissue optics, it is customary to distinguish between thin and thick media. For the thin media, the decay is governed by ballistic transport and, therefore, is simply analyzed using Beer's law. However, for the thick media, the light is heavily diffusive and is usually analyzed with the diffusion approximation. The specific route from ballistic to diffusive transport carries important information regarding the ability to see through the medium.

The transition regime has been the subject of several research studies, primarily for determining the limitations of the diffusion approximation analysis to describe particle and wave transports in thin slabs of random media. While $z/l_t \gg 1$ is considered as a valid region of the diffusion approximation, where z is the thickness of the media and l_t is the transport mean free path (TMFP), there is a lack of consensus and clarity regarding the lower bound of this region.

Although both Weitz et al.¹ and Freund et al.² applied the same method of diffuse wave spectroscopy, the former demonstrated that the photons were diffusive after a few TMFP, while the latter suggested the ballistic transport. Attempting to resolve this controversy, the experiment of Yoo et al.³ focused on the temporal aspect of photon distribution and concluded that the transport deviates from the diffusion approximation for $z/l_t < 10$. Using the same time-resolved propagation method, Kop et al.⁴ reported deviation for $z/l_t < 8$. This finding was confirmed by Elaloufi et al.⁵ using numerical analysis to solve the time-dependent radiative transfer equation. It should be noted, however, that when Kop et al. measured the total transmission, as opposed to time-resolved propagation measurements, no deviation was observed.

Zhang et al.,⁶ using a technique that allowed separation of the ballistic and scattered components of the transmitted field, found an abrupt transition from the ballistic to diffusive behavior

where the sample thickness was $z/l_t = 3$. These authors conducted Monte-Carlo simulations demonstrating that the ballistic-to-diffusive transition occurs between three and four TMFP. However, they note that this finding is not universal since the transition regime depends on the source–detector geometry of the experiment.

Consideration of the various approaches and findings leads to some degree of confusion regarding the location of the transition from ballistic to diffusive transport. This situation raises the question of whether the conceptualization is erroneous, i.e., the assumption that the TMFP is the correct parameter for determining the location of the transition from ballistic to diffusive transport is incorrect. If the assumption is not correct, what are the factors that influence this transition?

In this article, we carry out a basic analysis of the problem, develop and test a model specifically for use in the field of tissue optics, and determine the variables that influence the ballistic-to-diffusive transition. Our earlier research reported an agreement of the model for alterations of the medium's absorption coefficient.⁷ The present study examines an important conclusion of this model, which is the ability to extend the ballistic regime by reducing the solid angle of the measurement device. Finally, the research findings were applied to the consideration of an optical imaging system built on the principles of the model.

2 Theory

Light experiences absorption and scattering in transition through turbid media. For biological tissues, the dominant phenomenon is that of scattering. When the absorption coefficient is negligible compared with the scattering coefficient, i.e., $\mu_a \ll \mu_s$, the ballistic light extracting the medium I_b can be described by the Beer–Lambert law

$$I_b = I_0 \exp(-\mu_s z), \quad (1)$$

where I_0 is the light entering the medium.

Address all correspondence to: Ziv Glasser, Ariel University, Department of Electrical and Electronic Engineering, Kiryat Hamada 4, Ariel 40700, Israel. Tel: +972-3-9066259; Fax: +972-3-9066394; E-mail: zivg@ariel.ac.il

When the light is heavily scattered, the ballistic component is negligible as compared with the scattered light at the exit of the medium, customarily described as a diffusive dissemination.

Since the intensity of diffuse light at each point is (on the average) proportional to the density, we can apply the diffusion equation to the intensity instead of the photon density. The results of this study show that this assumption is indeed valid. Thus, for a uniformly illuminated slab, the diffusion approximation gives the following expression for the scattered light, I_d , exiting the medium⁸

$$I_d = I_0 \exp[-\sqrt{3\mu_a(\mu'_s + \mu_a)}z] \equiv I_0 \exp(-\mu_{\text{eff}}z), \quad (2)$$

where $\mu_{\text{eff}} \equiv \sqrt{3\mu_a(\mu'_s + \mu_a)}$, the reduced scattering coefficient $\mu'_s = \mu_s(1 - g)$ and $g = \langle \cos \theta \rangle$ is the mean cosine of the scattering angle, also known as the anisotropy factor.

It should be noted that the expression in Eq. (2) describes propagation of diffused light, and it is clear that only after several scattering events following entry into the media is it possible to consider light as diffused. Therefore, some change in the primary intensity is to be expected.⁹ Reference to this issue will be made further in this article. The total intensity entering the detector is simply the superposition of the ballistic and diffusive lights.¹⁰ However, we must take into consideration that while the ballistic light propagates in the forward direction, the diffusive light spreads spherically in all directions. Therefore, the diffusive light that reaches the detector is just a portion of the total diffusive light and depends on the collection angle $\delta\Omega$. Therefore, the total intensity can be written as $I = I_b + (\delta\Omega/4\pi)I_d$, i.e.,⁷

$$\frac{I}{I_0} = \exp(-\mu_s z) + \frac{\delta\Omega}{4\pi} \exp(-\mu_{\text{eff}} z). \quad (3)$$

In the literature, a third type of photon is present, which may play a role in the transition, namely, the snake photons.¹¹ Nevertheless, snake photons as separate entities are absent in Eq. (3). However, as it is evident from the comparison with the experimental results and as shown analytically by Rocco et al.,¹² it seems that such a term is not required (at least in the precision of the present experiment). This may be due to the fact that their quantity is negligible in comparison with the other components. Alternatively, the diffusion approximation may actually include the snake photons.

From the model, it is possible to extract the thickness z_c , at which the ballistic and the diffusive lights are equal, often called the transition width

$$z_c \equiv \frac{1}{\mu_s - \mu_{\text{eff}}} \ln\left(\frac{4\pi}{\delta\Omega}\right). \quad (4)$$

The zone $z < z_c$ is the ballistic regime, where the light entering the detector is mostly ballistic; thus, for slabs narrower than z_c , it is possible to achieve a good image of the sample. From Eq. (4), it can be concluded that the ballistic regime in the field of optical imaging (which we can usually assume $\mu_s \gg \mu_{\text{eff}}$) depends mainly on two parameters: the collection angle of the detector $\delta\Omega$ and the scattering coefficient μ_s . In addition, since in tissue optics $\mu_a \ll \mu_s$, the influence of the absorption coefficient on the location of the ballistic-to-diffusive transition is negligible. Therefore, when choosing the working wavelength λ , an important consideration is to choose a wavelength in which

the scattering coefficient is lower, even if the absorption coefficient for the particular wavelength is higher.

The other parameter to be considered in order to achieve a larger ballistic regime, aside from sample parameters, is the set of experimental conditions. For example, decreasing the collection angle $\delta\Omega$ would extend the ballistic regime. However, there is a limit; when the angle is progressively decreased, we finally reach the initial Gaussian beam diffraction angle $\delta\Omega = \pi a \tan^2(2\lambda/\pi d) \cong \pi(2\lambda/\pi d)^2$ (where d is the diameter of the initial beam), and further narrowing will reduce the ballistic and diffusive components at the same rate. Therefore, the maximum sample thickness for ballistic imaging (without any other filtering, of course) is defined as⁷

$$z_c^{\text{max}} \equiv \frac{2}{\mu_s - \mu_{\text{eff}}} \ln\left(\frac{d\pi}{\lambda}\right) \cong \frac{2}{\mu_s} \ln\left(\frac{d\pi}{\lambda}\right). \quad (5)$$

(since in tissue $\mu_s \gg \mu_{\text{eff}}$ is usually fulfilled). It should be noted that increasing the diameter of the beam increases the maximum width of the ballistic regime; however, this degrades the resolution of the image.

These two experimental features, i.e., the solid angle and the diameter of the incident beam, point to the advantage of collimated illumination, which involves the use of collimators at the entrance and exit of the medium.^{13,14} These collimators ensure a wide beam at the entrance and small ballistic angular diffraction at the exit.

3 Experiment

In order to validate the model a simple setup was used, as shown in Fig. 1.

The source used in this experiment was an 840-nm narrow-band CW laser. The medium was a solution of diluted Intralipid (5%), which is often used as a tissue phantom. The scattering coefficient for this concentration, according to our measurements, is $\mu_s \cong 82 \text{ cm}^{-1}$, and the reduced scattering coefficient is $\mu'_s \cong 15 \text{ cm}^{-1}$. We assume that the absorption coefficient is the same as 95% pure water, which is $\mu_a \cong 0.04 \text{ cm}^{-1}$. The collection angle was governed by the distance of the detector from the sample.

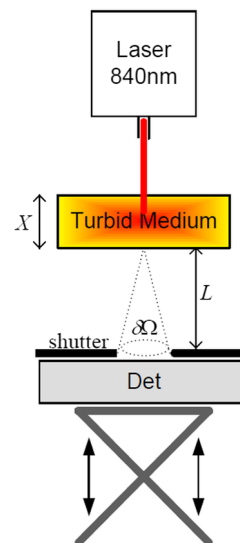


Fig. 1 Schematic illustration of the experiment.

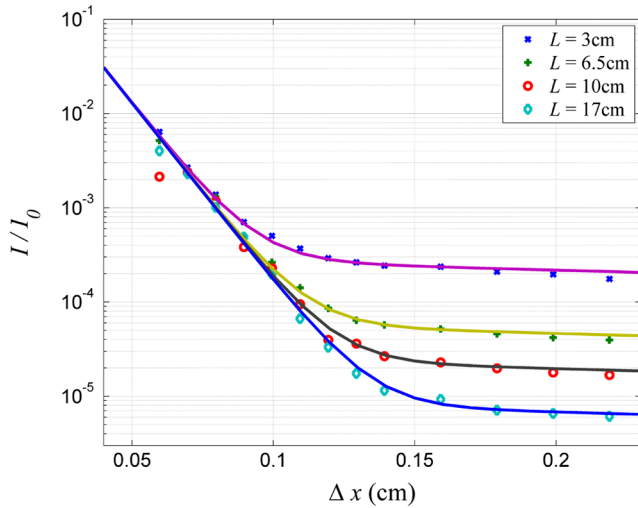


Fig. 2 Dependence of the transmission through the diffusive medium versus sample width (Δx) for various distances of the detector (L). The solid lines are a fit to Eq. (7).

Four sets of measurements were taken, where in each set, the detector distance from the sample changed. In each set, the thickness of the sample was increased gradually, and the transmission was measured through an aperture covering the detector. The diameter of the aperture was $D = 0.25$ cm, and thus, the collection angle depended only on the interval L between the sample and the detector. Therefore, the amount of diffusive photons collected by the detector, assuming spherical spread, is given by

$$\frac{\delta\Omega}{4\pi} \cong \frac{\pi D^2/4}{4\pi L^2} = \left(\frac{D}{4L}\right)^2. \quad (6)$$

The measured results were fitted into the following equation:

$$\frac{I}{I_0} = \exp(-\mu_s z) + \varepsilon \exp(-\mu_{\text{eff}} z), \quad (7)$$

using the same scattering and the absorption parameters for all four sets. Figure 2 presents the experimental results and the fitted function for each set.

By deducing the solid angle from Eq. (6), the results as plotted in Fig. 3(a) show the logarithmic increase in transition depth for reduction of the solid angle, as expected from our model. The factor ε was estimated from the fit (hereafter termed as ε_{exp}) for each set of measurements and compared with the reduction factor of the collection angle $\varepsilon_{\text{theor}} \equiv \frac{\delta\Omega}{4\pi}$. The results are presented in Fig. 3(b).

It was found that the theoretical and experimental values of ε are on the same order of magnitude and have the same dependence on the distance L , however, there is a discrepancy by a factor of 3. It is likely that this is due to the fact that the intensity of the diffusion component does not follow Eq. (2) at the point at which it enters the medium, but only after several scattering events. Hence, a certain factor (less than an order of magnitude) is needed to fix the boundary condition. Although the nature of the discrepancy is not clear, this graph evidently validates Eq. (3).

Another experiment using fiber collimators was conducted in which the source was a fiber-coupled diode-laser operating at

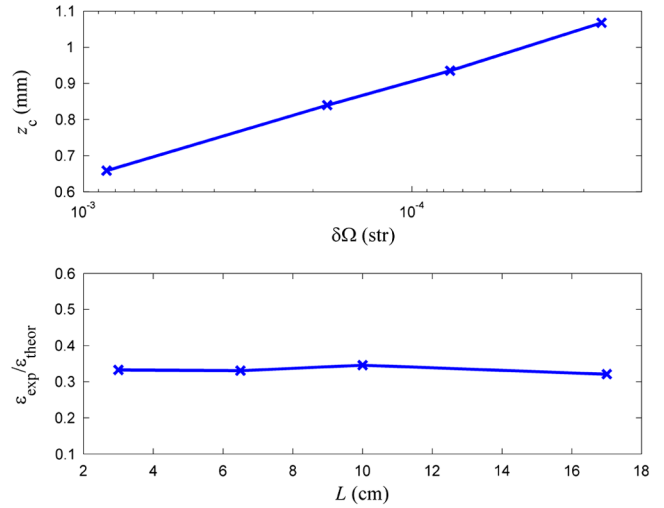


Fig. 3 (a) Transition depth z_c versus solid angle. (b) The ratio between the experimental and predicted ε versus distances of the detector (L).

1310 nm with a collimated beam. The advantage of using this wavelength is the relative lower-scattering coefficient.^{15,16} Although absorption is two orders of magnitude stronger, mostly, due to water molecules,¹⁷ the penetration depth of ballistic light is higher.

Instead of using an aperture before the detector, we used a fiber collimator with a focal length $f = 15.52$ mm. The fiber attached to the collimator was a multimode fiber with a core of $200 \mu\text{m}$, which leads to $\varepsilon_{\text{theor}} \cong 1 \cdot 10^{-5}$, whereas without the collimator, $\varepsilon_{\text{theor}} \cong 2.3 \cdot 10^{-2}$. The results were fitted into Eq. (7) and are presented in Fig. 4. The experimental ε with the collimator was found to be $\varepsilon_{\text{exp}} \cong 4 \cdot 10^{-5}$ and without the collimator, $\varepsilon_{\text{exp}} \cong 1.2 \cdot 10^{-2}$. In this experiment, ε_{exp} is also of the same order of magnitude as $\varepsilon_{\text{theor}}$. However, while without the collimator, ε_{exp} is lower than $\varepsilon_{\text{theor}}$ as in the previous experiment, with the collimator ε_{exp} was found to be higher than $\varepsilon_{\text{theor}}$ by a factor of 4. The reason for this is unclear. The ballistic regime was extended to 0.36 cm, which does not exceed the

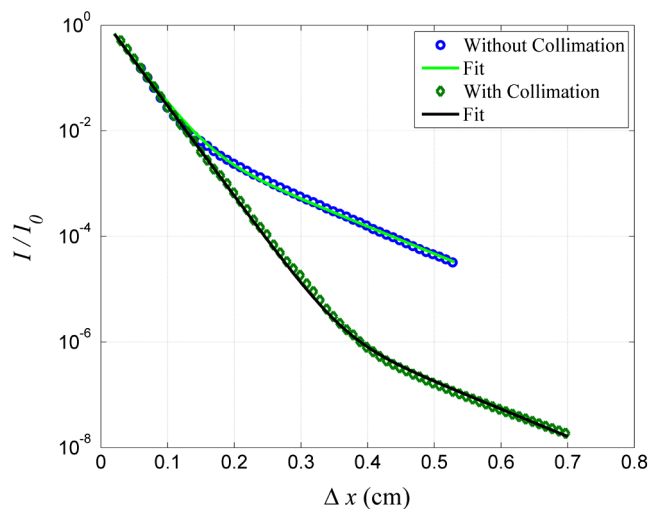


Fig. 4 Dependence of the transmission through the diffusive medium versus sample width (Δx) with and without a collimator at the exit of the sample. The solid lines are a fit to Eq. (7).

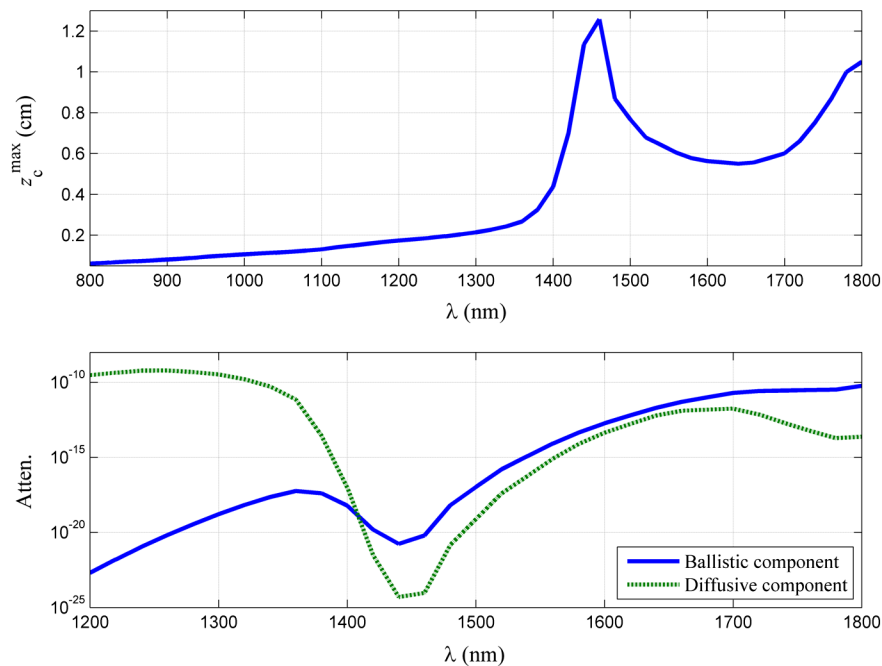


Fig. 5 (a) Maximum width for ballistic imaging versus wavelength for Intralipid 10%. (b) Attenuation of ballistic and diffusive components for sample thickness of 5 mm.

maximum width for ballistic imaging, which in this case is $z_c^{\max} \cong 0.7$ cm.

Finally, Fig. 4 shows that the ballistic regime in this setup was more than doubled by adding a simple collimator. In this experiment, the medium was Intralipid 10% with a reduced scattering coefficient of $\mu_s' |_{\lambda=1310} \cong 35$ cm^{-1} , which is between two and five times higher than that of skin tissue at 1300 nm.^{15,18}

For media with known optical parameters, one can use the analysis described above to derive the optimum operating wavelength, which will give the largest ballistic depth. However, the largest safe exposure and the smallest detectable intensities must be taken into consideration. As an example, Fig. 5(a) shows the maximum transition width (z_c^{\max}) for the emulsion of Intralipid 10% for an incident beam of 1 mm, as calculated from Eq. (5) given the following relevant optical parameters for the emulsion: (a) the scattering and the anisotropic coefficients were taken from the approximation of van Staveren et al.¹⁹ and (b) the absorption coefficient is the absorption of water,¹⁷ which is 90% of the solution. The maximum depth is obtained at a wavelength of 1460 nm, as a result of the absorption peak of water. This results in narrowing the gap between μ_s and μ_{eff} . However, it is useless to work at this wavelength because of the large loss of intensity. Therefore, the maximum loss of the system must be estimated in order to choose the appropriate wavelength.

Choosing the length of the sample (of Intralipid 10%) to be 5 mm, Fig. 5(b) shows the attenuation of the ballistic and the diffusive components of the detected intensity. Beyond the wavelength of 1.4 μm , the ballistic component is dominant compared with the diffusive component; however, below 1.6 μm , the large attenuation of the ballistic component poses a problem. In the wavelength regime between 1.6 to 1.8 μm , the loss of the ballistic component is about 10^{-11} , so that for an incident power of 10 mW (which is the maximum permissible exposure of skin for a surface of a square millimeter in this regime), a femtowatt-sensitive photoreceiver can detect the signal. According to our quantitative analysis, the advantage

of working in this wavelength regime is the improvement in the penetration depth for imaging.^{20–23}

This analysis leads to the conclusion that by choosing the appropriate wavelength and preparing the experimental conditions properly, it should be possible to extract the ballistic image of a tissue with a thickness of 1 cm or even more. In order to apply this method to an actual imaging system, it is necessary to develop the ability to process numerous pixels in a short time. This can be accomplished by an array of collimated illuminators.

4 Discussion

The current study was based on, and intended to further investigate, the findings of our earlier research. In our previous work, we presented a simple model to describe the quantitative relationship between ballistic and diffusive lights transmitted through random media, with a focus on the dependence of the absorption coefficient, and showed good agreement with experiment.⁷ In this article, the dependence of the transition depth on the illumination and detection conditions was experimentally validated. Calculations performed by Rocco et al. have shown agreement with these findings.¹²

Kempe et al.²⁴ also attempted to determine the ratio of ballistic to diffusive light, in order to achieve a maximum ballistic regime for confocal imaging systems. Experimenting with a suspension of latex spheres, they found similar behavior to that found in the current study. However, they do not take the absorption coefficient into account. According to their model, the ballistic–diffusive transition depends primarily on the sample’s parameters and aberrations, while in our model, in addition to the sample parameters, the main factor is the solid angle.

The findings of this research empirically confirmed the importance of this factor. This important conclusion provides us with the ability to expand the ballistic regime and can be realized with an imaging system based on an array of collimators to image through a tissue of 1-cm thickness.

It is important to note that in tissue, usually $\mu_s \gg \mu_{\text{eff}}$, so that the mean free path is of major significance as compared with the TMFP. Therefore, the transition is independent of the anisotropy factor g , which means that the TMFP is not the appropriate scaling parameter to determine the transition width. This is a significant finding of the present research, as it reflects on the basic conceptualization of the factors influencing transition.

References

1. D. A. Weitz et al., “Nondiffusive Brownian motion studied by diffusing-wave spectroscopy,” *Phys. Rev. Lett.* **63**(16), 1747–1750 (1989).
2. I. Freund, M. Kaveh, and M. Rosenbluh, “Coherent backscattering of light in a quasi-two-dimensional system,” *Phys. Rev. Lett.* **60**(10), 1214–1217 (1988).
3. K. M. Yoo, F. Liu, and R. R. Alfano, “When does diffusion approximation fail to describe photon transport in random media?,” *Phys. Rev. Lett.* **64**(22), 2647–2650 (1990).
4. R. H. J. Kop et al., “Observation of anomalous transport of strongly multiple scattered light in thin disordered slabs,” *Phys. Rev. Lett.* **79**(22), 4369–4372 (1997).
5. R. Elaloufi, R. Carminati, and J.-J. Greffet, “Diffusive-to-ballistic transition in dynamic light transmission through thin scattering slabs: a radiative transfer approach,” *J. Opt. Soc. Am. A* **21**(8), 1430–1437 (2004).
6. Z. Q. Zhang et al., “Wave transport in random media: the ballistic to diffusive transition,” *Phys. Rev. E* **60**(4), 4843–4850 (1999).
7. A. Yaroshevsky et al., “Transition from the ballistic to the diffusive regime in a turbid medium,” *Opt. Lett.* **36**(8), 1395–1397 (2011).
8. L. I. Grossweiner, *The Science of Phototherapy*, CRC Press, Tokyo (2011).
9. S. L. Jacques, “Simple theory, measurements, and rules of thumb for dosimetry during photodynamic therapy,” *Proc. SPIE* **1065**, 100–108 (1989).
10. K. M. Yoo and R. R. Alfano, “Time-resolved coherent and incoherent components of forward light scattering in random media,” *Opt. Lett.* **15**(6), 320–322 (1990).
11. L. Wang et al., “Ballistic 2-D imaging through scattering walls using an ultrafast optical Kerr gate,” *Science* **253**, 769–771 (1991).
12. H. O. Di Rocco et al., “Modeling transition diffusive–nondiffusive transport in a turbid media and application to time-resolved reflectance,” *J. Quant. Spectrosc. Radiat. Transfer* **120**, 16–22 (2013).
13. G. Jarry et al., “Imaging mammalian tissues and organs using laser collimated transillumination,” *J. Biomed. Eng.* **6**, 70–74 (1984).
14. A. O. Wist, P. P. Fatouros, and S. L. Herr, “Increased spatial resolution in transillumination using collimated light,” *IEEE Trans. Med. Imaging* **12**(4), 751–757 (1993).
15. A. N. Bashkatov, E. A. Genina, and V. V. Tuchin, “Optical properties of skin, subcutaneous, and muscle tissues: a review,” *J. Innov. Opt. Health Sci.* **4**(1), 9–38 (2011).
16. C. Chen et al., “A primary method for determination of optical parameters of turbid samples and application to intralipid between 550 and 1630 nm,” *Opt. Express* **14**(16), 7420–7435 (2006).
17. G. M. Hale and M. R. Querry, “Optical constants of water in the 200 nm to 200 μm wavelength region,” *Appl. Opt.* **12**(3), 555–563 (1973).
18. T. L. Troy and S. N. Thennadil, “Optical properties of human skin in the near infrared wavelength range of 1000 to 2200 nm,” *J. Biomed. Opt.* **6**(2), 167–176 (2001).
19. H. G. van Staveren et al., “Light scattering in Intralipid-10% in the wavelength range of 400–1100 nanometers,” *Appl. Opt.* **30**(31), 4507–4514 (1991).
20. B. E. Bouma et al., “Optical coherence tomographic imaging of human tissue at 1.55 μm and 1.81 μm using Er- and Tm-doped fiber sources,” *J. Biomed. Opt.* **3**(1), 76–79 (1998).
21. A. W. Sainter, T. A. King, and M. R. Dickinson, “Effect of target biological tissue and choice of light source on penetration depth and resolution in optical coherence tomography,” *J. Biomed. Opt.* **9**(1), 193–199 (2004).
22. U. Sharma, E. W. Chang, and S. H. Yun, “Long-wavelength optical coherence tomography at 1.7 μm for enhanced imaging depth,” *Opt. Express* **16**(24), 19712–19723 (2008).
23. V. M. Kodach et al., “Quantitative comparison of the OCT imaging depth at 1300 nm and 1600 nm,” *Biomed. Opt. Exp.* **1**(1), 176–185 (2010).
24. M. Kempe et al., “Ballistic and diffuse light detection in confocal and heterodyne imaging systems,” *J. Opt. Soc. Am. A* **14**(1), 216–223 (1997).